# MODELLING OF DUCTILE ANISOTROPIC CONTINUUM DAMAGE: EXPERIMENTS AND NUMERICAL ANALYSES

Michael Brünig
Lehrstuhl für Baumechanik-Statik, University of Dortmund, 44221 Dortmund, Germany

ABSTRACT
The paper deals with the continuum modelling of the large strain elastic-plastic deformation behavior of anisotropically damaged ductile metals. Damaged and undamaged configurations are introduced and the model is based on a kinematic description of damage. Different elastic potential functions allow to take into account the effect of damage on the elastic material properties. A generalized yield condition is employed to describe the plastic flow characteristics of the matrix material whereas the damage criterion provides a realistic representation of material degradation. Identification of material parameters is discussed in some detail. The applicability of the proposed continuum damage theory is demonstrated by numerical simulation of the inelastic deformation process of tension specimens of ductile materials.

## 1 INTRODUCTION

The accurate and realistic description of inelastic behavior of ductile materials as well as the development of associated efficient and stable numerical solution techniques are essential for the solution of boundary-value problems occurring in mechanical and civil engineering. An important issue in damage mechanics is the appropriate choice of the physical nature of mechanical variables describing the damage state of materials. It is well known from metallurgical tests that ductile fracture mainly occurs due to void nucleation, growth and coalescence which might lead to the formation of a mesocrack. From practical point of view continuum models intended to represent anisotropic damage phenomena should be simple enough to allow efficient numerical treatment and identification of material parameters but at the same time its simplicity should not eliminate the essential features of the numerical behavior within the range of application. Therefore, based on the concepts of continuum damage mechanics an efficient constitutive model is proposed and identification of material parameters as well as some numerical examples are discussed.

## 2 FUNDAMENTAL GOVERNING EQUATIONS

The framework presented by Brünig [1, 2] is used to describe the inelastic deformations including anisotropic damage due to microdefects. Briefly, the kinematic description employs the consideration of damaged as well as fictitious undamaged configurations related via metric transformations which allow for the definition of damage strain tensors $\mathbf{A}^{da}$. The modular structure is accomplished by the kinematic decomposition of strain rates, $\dot{\mathbf{H}}$, into elastic, $\dot{\mathbf{H}}^{el}$, effective plastic, $\dot{\bar{\mathbf{H}}}^{pl}$, and damage parts, $\dot{\mathbf{H}}^{da}$.

To be able to address equally to the two physically distinct modes of irreversible changes, i.e. plastic flow and damage, respective Helmholtz free energy functions with respect to the fictitious undamaged and to the current damaged configurations are introduced separately. The effective specific free energy $\bar{\phi}$ of the undamaged matrix material is assumed to be additively decomposed into an effective elastic and an effective plastic part

$$\bar{\phi} = \bar{\phi}^{el}\left(\bar{\mathbf{A}}^{el}\right) + \bar{\phi}^{pl}\left(\gamma\right) \tag{1}$$

where $\bar{\mathbf{A}}^{el}$ is the effective elastic strain tensor and $\gamma$ denotes an internal plastic variable. This leads in the case of isotropic elastic material behavior to the effective stress tensor

$$\bar{\mathbf{T}} = 2G\,\bar{\mathbf{A}}^{el} + \left(K - \frac{2}{3}G\right)\mathrm{tr}\bar{\mathbf{A}}^{el}\,\mathbf{1} \tag{2}$$

where $G$ and $K$ represent the shear and bulk modulus of the matrix material, respectively. In addition, plastic yielding of the hydrostatic stress-dependent matrix material is assumed to be adequately described by the yield condition

$$f^{pl}\left(\bar{I}_1, \bar{J}_2, c\right) = \sqrt{\bar{J}_2} - c\left(1 - \frac{a}{c}\bar{I}_1\right) = 0 \ , \tag{3}$$

where $\bar{I}_1 = \mathrm{tr}\bar{\mathbf{T}}$ and $\bar{J}_2 = \frac{1}{2}\mathrm{dev}\bar{\mathbf{T}} \cdot \mathrm{dev}\bar{\mathbf{T}}$ are invariants of the effective stress tensor $\bar{\mathbf{T}}$, $c$ denotes the strength coefficient of the matrix material and $a$ represents the hydrostatic stress coefficient. In elastic-plastically deformed and damaged metals irreversible volumetric strains are mainly caused by material damage and, in comparison, volumetric plastic strains are negligible. Thus, the plastic potential function

$$g^{pl} = \sqrt{\bar{J}_2} \tag{4}$$

depends only on the second invariant of the effective stress deviator which leads to the isochoric effective plastic strain rate

$$\dot{\bar{\mathbf{H}}}^{pl} = \dot{\lambda}\frac{\partial g^{pl}}{\partial \bar{\mathbf{T}}} = \dot{\lambda}\frac{1}{2\sqrt{\bar{J}_2}}\mathrm{dev}\bar{\mathbf{T}} \ . \tag{5}$$

Moreover, experiments reported by Spitzig et al. [3] have shown that the existence of microdefects results in a decrease of the stress level in the aggregate and in a decrease of the elastic material properties when compared to the response of the virgin undamaged material. Therefore, the Helmholtz free energy function of the damaged material sample is assumed to consist of three parts:

$$\phi = \phi^{el}\left(\mathbf{A}^{el}, \mathbf{A}^{da}\right) + \phi^{pl}(\gamma) + \phi^{da}(\mu) \ . \tag{6}$$

Namely, the elastic free energy $\phi^{el}$, which is an isotropic function of the elastic and damage strain tensors, $\mathbf{A}^{el}$ and $\mathbf{A}^{da}$, is used to describe the elastic response of the damaged material at the current state of deformation and material damage [4]. The energies $\phi^{pl}$, due to plastic hardening, and $\phi^{da}$, due to damage strengthening, only take into account the respective internal state variables, $\gamma$ and $\mu$. The elastic constitutive equation then yields the Kirchhoff stress tensor

$$\mathbf{T} = 2\left(G + \eta_2 \mathrm{tr}\mathbf{A}^{da}\right)\mathbf{A}^{el} + \left[\left(K - \frac{2}{3}G + 2\eta_1 \mathrm{tr}\mathbf{A}^{da}\right)\mathrm{tr}\mathbf{A}^{el} + \eta_3\left(\mathbf{A}^{da} \cdot \mathbf{A}^{el}\right)\right]\mathbf{1}$$
$$+ \eta_3 \mathrm{tr}\mathbf{A}^{el}\mathbf{A}^{da} + \eta_4\left(\mathbf{A}^{el}\mathbf{A}^{da} + \mathbf{A}^{da}\mathbf{A}^{el}\right) \quad (7)$$

which is linear in $\mathbf{A}^{el}$ and $\mathbf{A}^{da}$, and $\eta_1 ... \eta_4$ are newly introduced material constants taking into account the deterioration of the elastic material properties due to damage.

Furthermore, in analogy to the yield surface and flow rule concepts employed in plasticity theory, evolution of damage is assumed to be adequately described by the damage criterion

$$f^{da}\left(I_1, J_2, \tilde{\sigma}\right) = I_1 + \tilde{\beta}\sqrt{J_2} - \tilde{\sigma} = 0 \quad (8)$$

where $\tilde{\beta}$ represents the influence of the deviatoric stress state on the damage condition and $\tilde{\sigma}$ denotes the equivalent damage stress measure. In addition, the damage potential function

$$g^{da}\left(\tilde{\mathbf{T}}\right) = \alpha I_1 + \beta\sqrt{J_2} \quad (9)$$

with kinematically based damage parameters $\alpha$ and $\beta$ leads to the damage rule

$$\dot{\mathbf{H}}^{da} = \dot{\mu}\alpha\mathbf{1} + \dot{\mu}\beta\frac{1}{2\sqrt{J_2}}\mathrm{dev}\,\tilde{\mathbf{T}} \quad (10)$$

where the first term represents inelastic volumetric deformations caused by further isotropic growth of microvoids whereas the second term takes into account the dependence of the evolution of shape and orientation of microdefects on the direction of stress.

## 3 EXPERIMENTS AND MATERIAL PARAMETERS

Identification of continuum models consists in the quantitative evaluation of the chosen material coefficients. Therefore, Spitzig et al. [3] performed a large number of systematic experiments on iron compacts of different initial porosities. These data are used here to determine the material parameters of the proposed anisotropic damage model. In particular, the elastic constants of the matrix material are chosen to be $G$ = 81300 MPa and $K$ = 166270 MPa. The nonlinear increase of the current strength coefficient $c$ appearing in the yield condition (3) is numerically characterized by the power law

$$c = c_0\left(\frac{H_0\gamma}{n\ c_0} + 1\right)^n \quad . \quad (11)$$

The initial yield strength $c_0$ = 57.74 MPa, the initial hardening parameter $H_0$ = 5500 MPa, and the hardening exponent $n$ = 0.296 give the best fit to experimental values. In addition, numerical analyses presented by Tvergaard and Needleman [6] suggested that during the increasing damage process the aggregate stress falls slowly until the void volume fraction reaches the critical value $f_c$ and, then, it drops abruptly with a remarkable loss of stress carrying capacity. Motivated by these results the equivalent aggregate stress-equivalent damage strain curve is approximated by a bilinear relation where the respective slopes $H^{da} = \dfrac{d\sigma}{df}$ are chosen to be

$$H_1^{da} = -50\,\text{MPa} \quad \text{for} \quad f < f_c \tag{12}$$

and

$$H_2^{da} = -4000\,\text{MPa} \quad \text{for} \quad f \geq f_c \ . \tag{13}$$

Furthermore, the four additional material constants $\eta_1 ... \eta_4$ appearing in the elastic constitutive equation (7) which describe the deteriorating influence of increasing damage on the elastic properties of the aggregate are estimated by fitting four experimental elastic moduli-porosity curves [3]. The respective parameters are chosen to be $\eta_1$ = -117 500 MPa, $\eta_2$ = -95 000 MPa, $\eta_3$ = -190 000 MPa and $\eta_4$ = -255 000 MPa. For example, Figure 1 shows the comparison for the shear modulus, $G_d$, versus the current void volume fraction between experimental data and the predicted curves based on the chosen parameters discussed above. In particular, remarkable decrease of $G_d$ with increasing damage is observed in Fig. 1 and at $f$ = 0.111, $G_d$ attains about 75% of its initial value. The available experimental data given by Spitzig et al. [3] are accurately depicted by the analytical curve. Similar results are obtained concerning the reduction of Young's modulus, the bulk modulus and Poisson's ratio [1]. Hence, the proposed anisotropic damage model is verified to properly depict the results of the relevant tests.

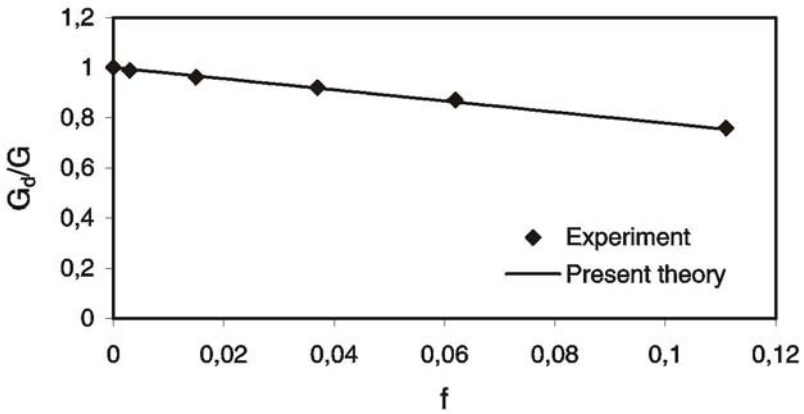


Figure 1: Effect of porosity on the shear modulus.

## 4 NUMERICAL EXAMPLE

The finite deformation behavior of uniaxially loaded rectangular specimens with clamped ends is numerically analyzed. The numerical calculations take into account plane strain conditions and are based on the elastic-plastic-damage model with the constitutive parameters discussed above. Figure 2 shows the load-deflection curve which first shows an increase in load with increasing elastic-plastic deformations due to the work- hardening characteristics of the iron matrix material discussed above. The load has a maximum at the elongation *u/l* = 0.157 which is followed by a small sudden decrease of only about 1% corresponding to the onset of damage at the critical equivalent plastic strain $\gamma_c = 0.2$ and a slight subsequent load increase. This effect of beginning void growth on the overall load-deflection behavior has also been observed in the numerical analyses reported by Tvergaard and Needleman [6]. From *u/l* = 0.188 a small decrease in load with increasing deformation is observed. Although the equivalent matrix stress- equivalent plastic strain curve (Eq. 11) still shows work-hardening behavior this slow decrease is due to the decrease in the current specimen's area as well as in the onset and growth of isotropic damage which results in decrease in aggregate stress. Then, at the elongation *u/l* = 0.412 an abrupt drop in load is predicted associated with a remarkable loss in load carrying capacity of the iron specimen. This fast decrease in load attributes to void coalescence and the subsequent formation and growth of microcracks thus leading to final fracture. This numerically predicted load-deflection behavior qualitatively agrees quite well with experiments and numerical calculations on ductile metal specimens reported by Tvergaard and Needleman [6] and with experimental observations presented by Lemaitre and Dufailly [7].

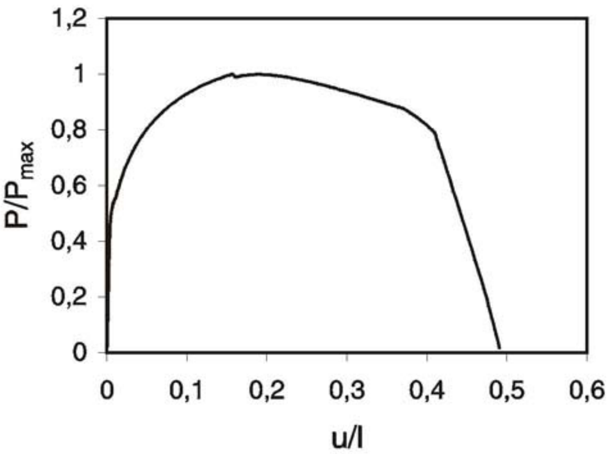


Figure 2: Load-deflection curve.

In addition, Fig. 3 illustrates the effect of the equivalent plastic strain on the current void volume fraction in a homogeneously deformed material element. In particular, after the onset of damage a nearly linear increase in porosity with increasing plastic deformation is observed. Afterwards, from $\gamma$ = 0.423 the current porosity starts to increase much more rapidly with increasing plastic deformations. This effect is due to further void growth and simultaneous void coalescence which leads to the formation of microcracks. This numerically predicted behavior is in good agreement with experimental results reported by Spitzig et al. [3].

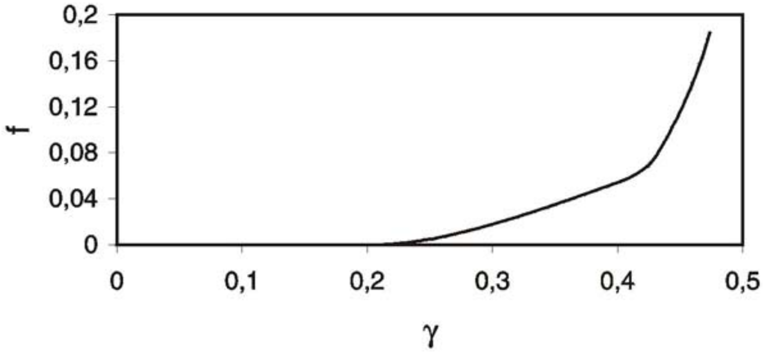


Figure 3: Current void volume fraction vs. equivalent plastic strain.

## 5 CONCLUSIONS

A numerical model for the analysis of ductile elastic-plastic-damage metals has been presented. A characteristic feature of the present phenomenological continuum approach is the consideration of damaged as well as fictitious undamaged configurations related via damage tensors. Respective free energy functions are introduced separately which allow the formulation of elastic constitutive laws for both the matrix material and the damaged aggregate. Since plastic flow and damage are distinctly different irreversible processes in their nature, plastic constitutive equations are formulated in an effective stress space whereas the evolution equation of the anisotropic damage strain rate tensor is given in the damaged aggregate stress space. The applicability of the proposed continuum damage theory has been demonstrated by the numerical simulation of the deformation behavior of ductile solids. Hence, the present model offers a complementary alternative to conventional fracture mechanics and provides a comprehensive theory of anisotropic continuum damage mechanics capable of solving practical engineering problems including service life prediction of metal structures.

## REFERENCES

1. M. Brünig, An anisotropic ductile damage model based on irreversible thermodynamics, Int. J. Plast., 19, (2003), 1679-1713.
2. M. Brünig, Numerical analysis of anisotropic ductile continuum damage, Comput. Meth. Appl. Mech. Engrg. 192, (2003), 2949-2976.
3. W.A. Spitzig, R.E. Smelser, O. Richmond, The evolution of damage and fracture in iron compacts with various initial porosities, Acta Metall., 36, (1988), 1201-1211.
4. K. Hayakawa, S. Murakami, Y. Liu, An irreversible thermodynamics theory for elastic-plastic-damage materials, Eur. J. Mech. A/Solids, 17, (1998), 13-32.
5. R. Becker, A. Needleman, O. Richmond, V. Tvergaard, Void growth and failure in notched bars, J. Mech. Phys. Solids, 36, (1988), 317-351.
6. V. Tvergaard, A. Needleman, Analysis of the cup-cone fracture in a round tensile bar, Acta Metall., 32, (1984), 157-169.
7. J. Lemaitre, J. Dufailly, Damage measurements, Eng. Frac. Mech., 28, (1987), 643-661.